Rock Mech. Rock Engng. (1999) 32 (2), 123–155

Rock Mechanics and Rock Engineering

Time-dependent Behaviour of Deep Level Tabular Excavations in Hard Rock

By

D. F. Malan

CSIR Mining Technology, Johannesburg, South Africa

Summary

Although hard rock is not usually associated with large creep deformation, significant time-dependent behaviour is observed in the tabular excavations of the South African gold mines. Time-dependent closure data was collected in stopes of the Ventersdorp Contact Reef and Vaal Reef. This data typically consists of a primary closure phase after blasting, followed by a steady-state closure phase. This closure behaviour is the result of the rheology of the fracture zone around these excavations and the time-dependent extension of this zone following a mining increment. An elasto-viscoplastic approach was developed to simulate the time-dependent nature of the fracture zone. This model proved successful in simulating the experimental closure profiles. It appears that the closure data may provide useful diagnostic information of the stress conditions in the fracture zone ahead of the face. This may possibly be used to identify hazardous conditions such as areas prone to face bursting. The effect of preconditioning on the time-dependent closure behaviour is also illustrated.

1. Introduction

1.1 The Need for Research into the Time-dependent Behaviour of Deep Excavations in Hard Rock

Changes in the local stress state due to mining activity perturb the stability of the rock mass surrounding excavations. The subsequent readjustment of the rock towards a new equilibrium does not occur instantaneously but as a gradual process over time. This process can include two types of inelastic deformation, namely creep-like movements and violent failures or rockbursts. Depending on the rock type and stress, excavations can show a propensity towards either of these two phenomena. In relation to mine safety it is therefore important to determine the conditions associated with the transition from stable deformation to rockbursts.

This paper investigates the time-dependent behaviour of the tabular excavations in the deep South African gold mines. Intuitively, one would not expect significant time-dependent rock behaviour in these mines as the creep rate of the intact hard rock is low. Contrary to this belief, appreciable time-dependent movements have been observed underground as illustrated in the next section. This study is an attempt to increase the understanding of the time-dependent behaviour of hard rock and to simulate it numerically.

To avoid confusion over the terms *creep* and *time-dependency*, the following definitions are introduced and will be used throughout this publication. *Creep* is continued deformation due to a constant applied stress and will be used exclusively in relation to intact laboratory-sized specimens containing no large scale discontinuities. *Time-dependency* will be used as a more general term encompassing concepts like the creep of intact rock, creep of large scale discontinuities, delayed failure and long term strength. As the rheological behaviour of the rock mass underground is a complex interrelation of these factors, it will therefore be referred to as time-dependent. Time-dependency is also understood to refer to deformations not related to geometric changes in the dimensions of an excavation. It occurs on a time scale of days to years and is therefore not related to elastodynamic behaviour.

For engineering applications, the importance of time-dependent behaviour in the form of rapid convergence of tunnels in weak rock is well known (Gioda, 1982; Panet, 1996). In comparison, creep strain in crystalline rock is of limited importance in most engineering projects due to the very low creep rate (Dusseault and Fordham, 1993). Researchers in the South African gold mining industry (Roux and Denkhaus, 1954; Denkhaus et al., 1958) nevertheless recognised that the time-dependent behaviour of hard rock is important as it may cast light on why rockbursts do not always occur at blasting time, but also when there is no external influence that could account for changes in stress distribution. The importance of including the time factor in analyses of instabilities in mines was recently emphasised by Linkov (1996). Significant time-dependent deformation is important as it may cause a gradual non-violent reduction of abutment stress and hence diminish the danger of rockbursts. Dusseault and Fordham (1993) noted that for the mining engineer, ongoing time-dependent deformation is an indication of the efficient redistribution of stress, preventing the build-up of large stress concentrations. Denkhaus et al. (1958) found that in South African mines the susceptibility to rockbursts was much more prevalent in stopes in the Central Rand, where the reef lies between hard brittle quartzite bands, than on the Far East Rand where the reef lies on ductile shale.

One strategy that may be useful in controlling the stability of the fracture zone in hard rock is the rate of stope face advance. Although not related to hard rock, Linkov (1996) noted that in the Kizel coal mines, doubling the rate of coal cutting on a face from 0.27 m/min to 0.54 m/min resulted in a drastic increase in the incidence of rockbursts. Cook et al. (1966) found from a statistical analysis of rockburst data in the South African mines that there is an increase in rockbursts for a face advance rate of more than 4 m a month for small abutments, to 8 m a month for large abutments. Hodgson (1967) predicted that if the face advanced faster

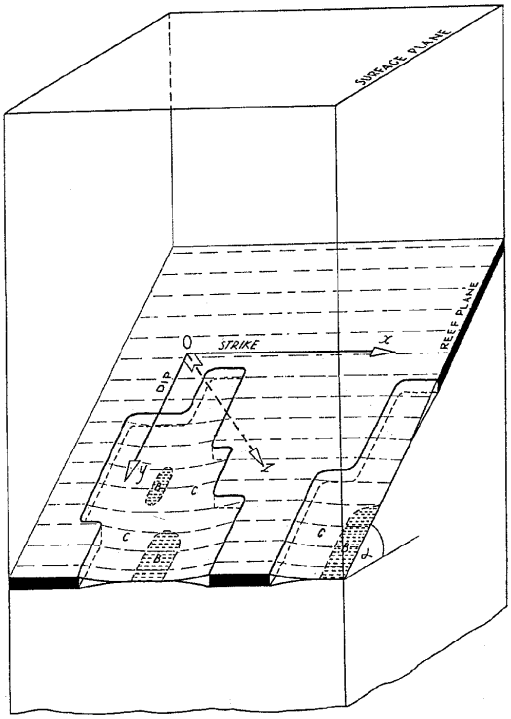

Fig. 1. Schematic diagram of a typical tabular ore body dipping at $\alpha°$ (after Salamon et al., 1964). Visible are mined regions (C) and areas of contact between the hangingwall and footwall (B)

than the time-dependent migration of the fracture zone ahead of the stope face, less energy would be released in a stable manner, thereby increasing the incidence of rockbursts. A time-dependent constitutive law appropriate to rock on a mine-wide scale could therefore lead to some generalisations regarding safe rates of extraction and better control of the fracture zone. Unfortunately, no complete understanding of the time-dependent behaviour of deep excavations in hard brittle rock has, as yet, been achieved.

1.2 Tabular Excavations of the South African Gold Mines

The gold-bearing conglomerates of the Witwatersrand system are essentially plane tabular in nature, implying a negligible height compared to the lateral extent of the orebody (Fig. 1). Although the reef is frequently dislocated by faults and dykes, the plane tabular nature of the orebody can persist for many square kilometres in some areas. Although the reef can be nearly horizontal in certain locations, it is generally inclined between 25° and 45° (*dip angle*). The reef thickness can vary from a few centimetres to more than a metre. In order to maintain economic viability, the reefs are mined with as small a working height or *stoping width* as possible. In 1980 the average stoping width throughout the industry was esti-

mated to be 1.33 m (Gay and Jager, 1980). Reef extraction may extend over several square kilometres resulting in large stope spans and eventual contact between the roof (*hangingwall*) and floor (*footwall*) of the excavations in the areas far from the working faces. The relative movement of the hangingwall and footwall normal to the plane of the reef is called *closure*. *Convergence* refers to the elastic component of closure. Closure is therefore the sum of elastic convergence and inelastic deformation. The average rock breaking depth is approximately 2000 m, although workings deeper than 3500 m can be found (Schweizer and Johnson, 1997). It is forecast that by the year 2010 some 30% of South African gold production will come from depths greater than 3000 m (Johnson and Schweizer, 1996). Typical virgin stresses encountered at a depth of 2500 m are 70 MPa in the vertical direction and 35 MPa in the horizontal direction.

A description of the most important gold-bearing reefs currently exploited can be found in Schweizer and Johnson (1997). The following two reef types are of interest in this study. The *Ventersdorp Contact Reef* (VCR) is an intermittent conglomerate at the base of the Ventersdorp Supergroup, with pebble sizes varying from a few millimetres to 40 cm. The footwall of these excavations in different areas consists of a great variety of quartzites ranging from siliceous to argillaceous. The hangingwall of the VCR is formed by volcanic rocks that can be divided into Westonaria Formation lavas (termed soft lava) and Alberton Porphyry Formation lavas (termed hard lava). The *Vaal Reef* is a conglomerate consisting of small pebbles closely packed in a pyritic matrix. It varies in width from a carbon parting to over 1.2 m. The footwall and hangingwall of the excavations in these areas consist of argillaceous to siliceous quartzites. The main rock types exposed by the tabular mining of these two reef types are therefore brittle quartzite and lava. The strength of these rocks varies greatly from area to area. The uniaxial (unconfined) compressive strength (UCS) of an average Witwatersrand quartzite is 200 MPa (Gay and Jager, 1980), although it can be as low as 130 MPa (Malan and Bosman, 1997). Some of the Alberton Porphyry lavas are very rigid and can have UCS values of more than 400 MPa. The laboratory creep rate of these quartzites and lavas are very low, as described in Malan (1998).

As a result of the great depth and the tabular nature of the excavations, large stresses are experienced ahead of the working faces. These normally exceed the strength of the rock, resulting in the formation of an extensive fracture zone. Under high stress conditions, this zone can extend to more than 5 m ahead of the face (Adams et al., 1981). After blasting, the fracture zone needs to adapt to the changing stress conditions. Little is known about the time-dependent nature of this process. Adams and Jager (1980) investigated the extent of the fracture zone and the pattern of rock failure that occurs ahead of advancing stope faces. They found the formation of fractures to be associated with the face advance, with the majority of new fractures forming within a relatively short period after blasting. The amount of new fracturing taking place diminished with time. Their observations indicated that if the face was not mined for a period of two weeks, no new fractures formed. Turner (1984) also observed time-dependent fracture development at a mechanized rock-breaking site at Doornfontein Gold Mine. He investigated the occurrence of hard patches in the face that were therefore difficult to mine using

mechanical equipment, owing to the absence of fracturing. It was noted that some of these patches became mineable after a few days as the rock became fractured. This time-dependent fracturing occurred even when no mining had taken place for several days. Legge (1984) made a series of measurements of displacements associated with the development and behaviour of fractures. Extensometer data indicated that new fractures initiated as narrow dilating zones some distance ahead of the face, in response to advances of 0.5 m or more. Continuous recordings of extensometer data indicated that the movements occurred in a time-dependent fashion that typically lasted up to nine hours after blasting. If stopes were not mined for extended periods, only the portion of the fracture zone close to the face (≤ 1 m) showed significant further time-dependent dilation. During one period at the mechanized rock-breaking site at Doornfontein Gold Mine, the panel was not mined for a month. The rock within 1.5 m of the face nevertheless experienced a further dilation of 10 mm in this period.

2. Time-dependent Closure Data

Time-dependent closure data of tabular excavations is a good reflection of the localised rock response and can provide important information which may be more difficult to obtain with other methods. Unfortunately this source of data has been largely neglected in the South African industry. Although a large number of closure measurements have been recorded (Wiggill, 1965; Gürtunca, 1989; King et al., 1989; Güler, 1997), these measurements usually consisted of measurements with a 24 hour interval or longer between successive data points. Data collected by Walsh et al. (1977) at West Driefontein Mine had an interval of a week between measurements. All these measurements will be collectively termed *long period* measurements. Typical results obtained from these measurements can be very difficult to interpret as the closure curves are the complex result of a) enlargement of the excavation, b) the face moving away from the measurement position and c) the true time-dependent behaviour of the rock mass. In spite of these problems, significant time-dependent rock behaviour was noted by some researchers. Hodgson (1967) analysed data from East Rand Proprietary Mines and noted significant time-dependent closure behaviour. He explained this behaviour as being caused by the time-dependent migration of the fracture zone ahead of the face, resulting in the effective stope span becoming bigger. King et al. (1989) measured closure behaviour in two adjacent panels at Hartebeestfontein Mine. After blasting activity had stopped in one of the panels, the closure rate in this panel continued at a constant rate of 6 mm/day for 37 days. Only after this period did the rate gradually start to decrease. Mining, however, continued in the second panel (and probably in other nearby panels) and the effect of these geometrical changes on the first panel is unclear. After mining stopped in the second panel, the closure rate in this panel persisted for thirteen days and then gradually declined. Closure data collected by Gürtunca (1989) in the Klerksdorp area, to quantify the effect of backfill, also exhibited significant time-dependent effects. Daily

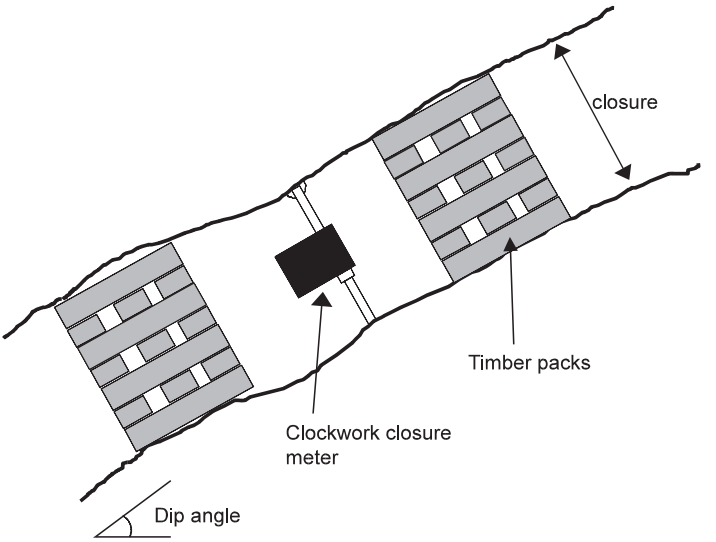

Fig. 2. Installation of the clockwork closure meter normal to the plane of the excavation

Table 1. Typical properties of the hangingwall and footwall rocks at Western Deep Levels Mine and Hartebeestfontein Mine. The abbreviations are: *UCS* Uniaxial compressive strength, *E* Young's modulus, *v* Poisson's ratio and ρ density. Note that these values might vary greatly from area to area

	UCS (MPa)	E (GPa)	*v*	ρ (kg/m^3)
Western Deep Levels Mine (VCR)				
Hangingwall lava	436	88	0.26	2902
Footwall quartzite	237	79	0.13	2710
Hartebeestfontein Mine (Vaal Reef)				
Hangingwall quartzite (Main Bird Series 4)	206	66	0.18	–
Footwall quartzite (Main Bird Series 5)	208	64	0.18	–

closure rates varied from panel to panel and were in some instances as high as 30 mm/day.

To analyse the true time-dependent behaviour of the rock mass, data for this study was collected using clockwork closure instruments which record the stope closure continuously. A description of these instruments can be found in Malan (1998). Figure 2 illustrates a typical installation of this instrument in a stope.

2.1 Closure Data of the Ventersdorp Contact Reef

Closure data was collected in the South Shaft area of Western Deep Levels Mine near Carletonville. The hangingwall of the Ventersdorp Contact Reef at this mine consists of hard lava. Some typical properties of the rocks in this area are given in Table 1. The general mining layout in this area is given in Fig. 3. The instrumen-

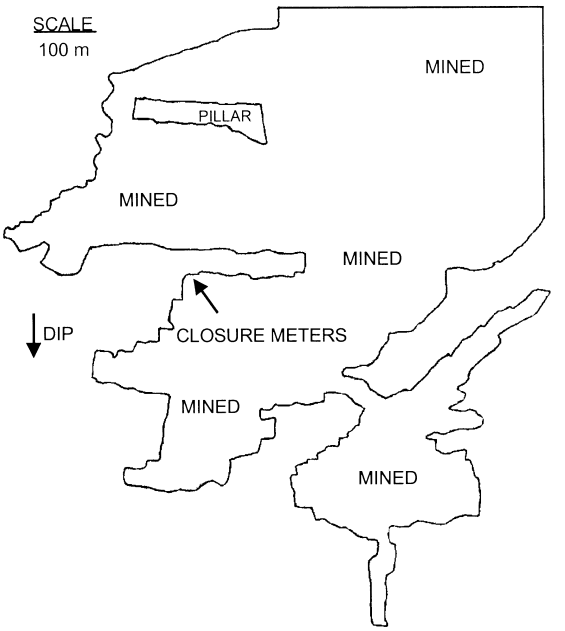

Fig. 3. Plan view of the mining geometry in the area where the closure data was collected at Western Deep Levels Mine

tation was installed in the W3 panel of the 87-49 longwall. An enlarged view of this panel is given in Fig. 4. The dip of the reef is 22° and the depth below surface is approximately 2570 m. Timber packs are used as back-area support in this panel. Five clockwork closure meters were installed at any one time, with their positions before the blast on 15/4/97 illustrated in Fig. 4. Typical recorded time-dependent closure is illustrated in Fig. 5. Note that there is a sudden increase in the closure after the blast consisting of an instantaneous jump and a period ($\approx$5 hours) of decelerating rate of closure. This will be called the primary closure. This is followed by a more gradual steady-state closure rate. If there is no mining activity for a number of days, the rate of steady-state closure appears to remain constant in the short term ($\approx$48 hours after the last blast), but then gradually starts declining until the next blast occurs. Typically, after a period of two weeks with no blasting, the rate of steady-state closure is reduced to 10% of its short term value. Of interest is that if seismic events occurred close to the panel, time-dependent closure behaviour similar to that after a blast is observed as depicted in Fig. 5. The magnitude of the primary closure after a seismic event is dependent on the magnitude of the event and how close its source was located to the panel. A further closure data set is given in Fig. 6.

After any particular blast, the increase in closure is a function of the distance to the face, position in the panel and length of face advance. Fig. 7 illustrates the incremental closure for stations no. 2, 4 and 5 (see Fig. 4) after the blast on 15/4/97. The primary closure is large close to the face, but smaller as the distance to the

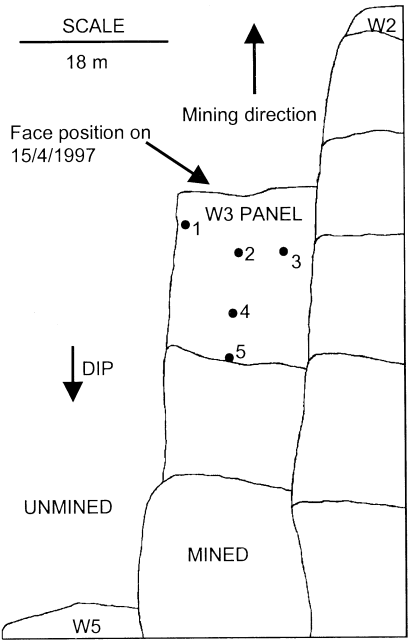

Fig. 4. Enlarged plan view of the W3 up-dip panel in the 87-49 longwall with the positions of the closure meters indicated

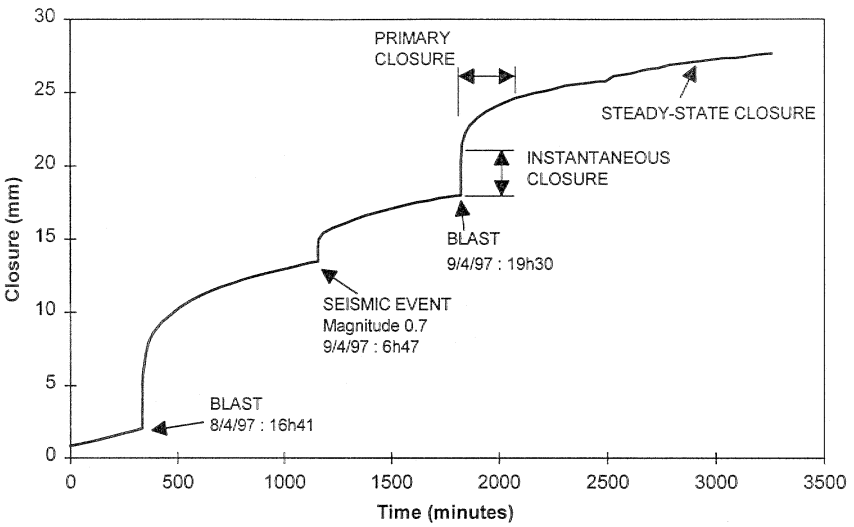

Fig. 5. Typical time-dependent stope closure of the Ventersdorp Contact Reef at Western Deep Levels Mine. This was for a closure station at a distance of 8.7 m from the face

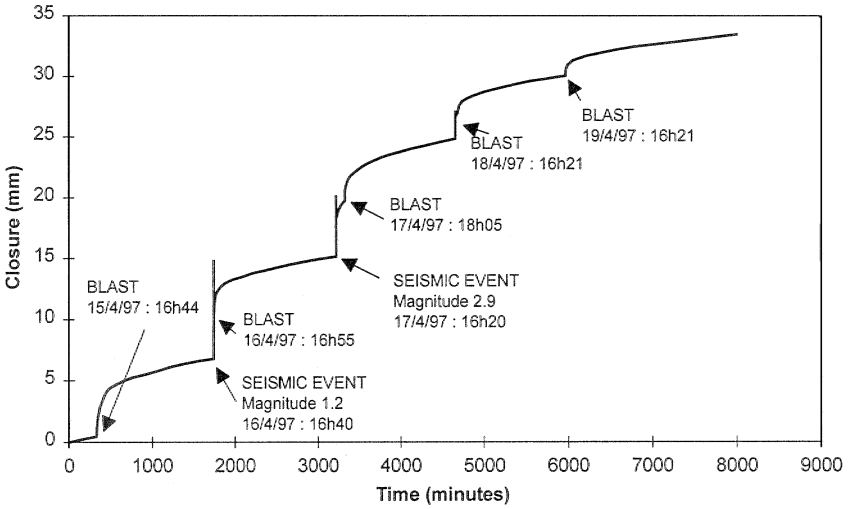

Fig. 6. Time-dependent closure measured at Western Deep Levels Mine. This was for instrument no. 1 which was 4.1 m from the face before the blast on 15/4/97. The overshoot behaviour after seismic events is a response of the closure meter due to dynamic loading and not a reflection of the true rock mass behaviour

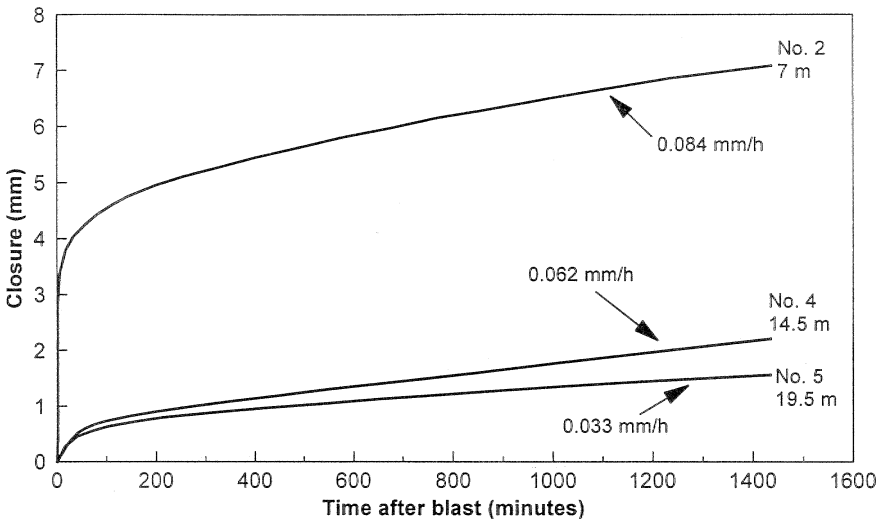

Fig. 7. Closure as a function of time for different positions in the panel following the blast on 15/4/97. The distances given in the graph are the distances from the closure instruments to the face before the blast (see Fig. 4)

face increases. The rate of steady-state closure also decreases into the back area. Figure 8 compares the behaviour after the same blast for the row of stations approximately parallel to the face (no. 1, 2 and 3). Although the steady-state closure rate is essentially similar for these three stations, the magnitude of primary closure

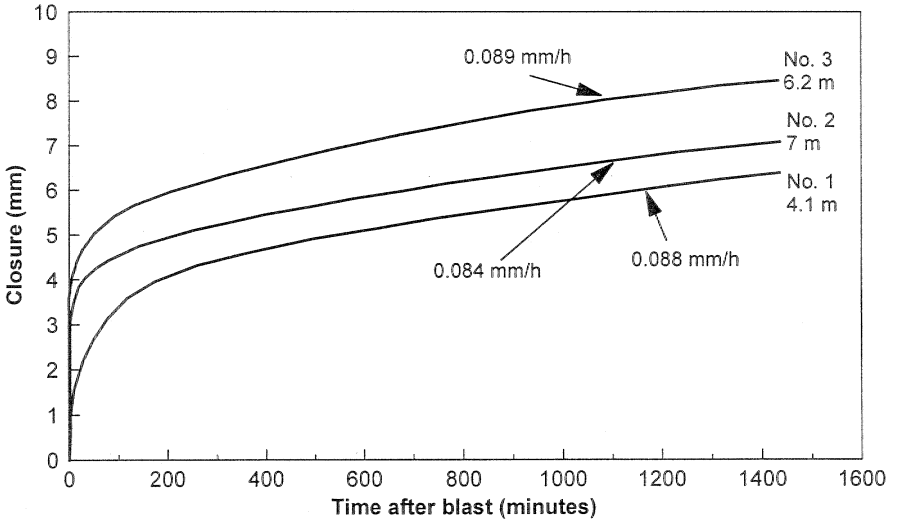

Fig. 8. Closure as a function of time for different positions approximately parallel to the face following the blast on 15/4/97. The distances given in the graph are the distances from the closure instruments to the face before the blast (see Fig. 4)

increases from the solid abutment (no. 1) to the previously mined side (no. 3) of the panel. As it is difficult to determine the onset of the steady-state closure phase, the closure rates given in Fig. 7 and Fig. 8 were calculated for a period from 600 minutes after the blast to the end of the data set. The dependence of the rate of steady-state closure on distance to face is further illustrated in Fig. 24 (Section 4). Note that this behaviour is only noted in Ventersdorp Contact Reef stopes where the hangingwall consists of hard lava (see Section 1.2 for a description of hard and soft lava). In areas where the lava is soft, measurements (not described in this study) indicate that the steady-state closure rate is much higher and the behaviour is more similar to the Vaal Reef described below. Note that any further reference to the behaviour of Ventersdorp Contact Reef stopes in this paper refers to those areas where the hangingwall consists of hard lava.

2.2 Closure Data of the Vaal Reef

To contrast the relatively low closure rates of the Ventersdorp Contact Reef with areas experiencing significant closure, data was collected from the No. 6 shaft pillar area at Hartebeestfontein Mine in the Klerksdorp area. Some typical properties of the rocks in this area are given in Table 1. A schematic diagram of the shaft pillar area is given in Fig. 9. A single closure meter was installed in the position illustrated in Fig. 10. The dip in this area was 7° and the depth approximately 2350 m. Timber packs were used as back-area support in this panel. This shaft area is known to have very high closure rates. Of significance are the well-defined bedding planes in the quartzite. The nature of infilling of these dis-

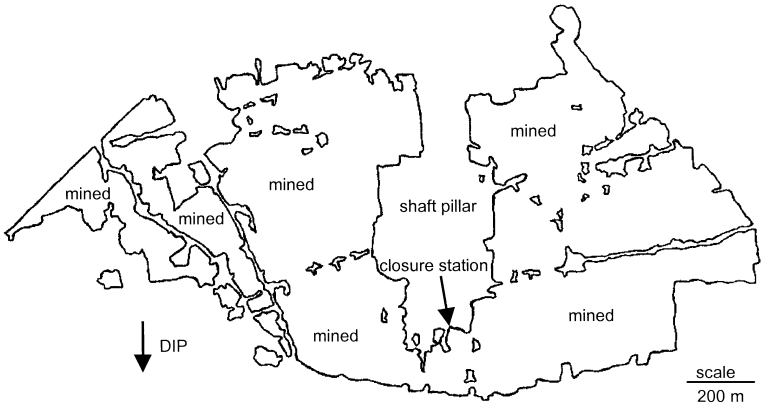

Fig. 9. Plan view of the mining geometry at No. 6 shaft pillar area, Hartebeestfontein Mine, where the closure data was collected.

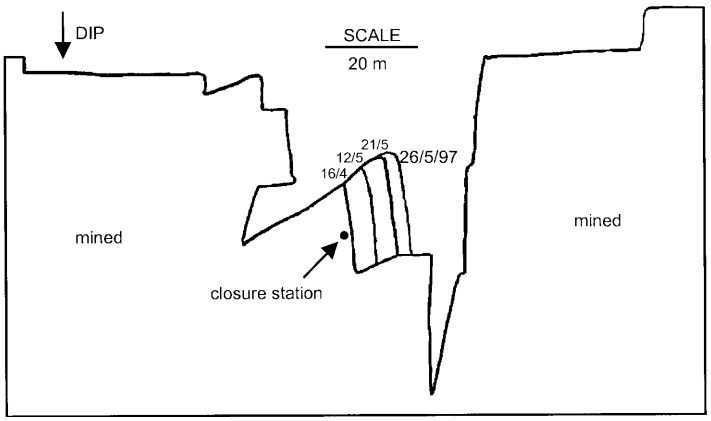

Fig. 10. Location of the clockwork closure instrument in the 78N23 longwall at No. 6 shaft, Hartebeestfontein Mine

continuities makes conditions less favourable for stable mining excavations. The overall competency of the rock mass and its ability to provide stable mining excavations for prolonged periods appears to be less favourable than the rock types encountered in Ventersdorp Contact Reef mining operations. The quartzites of the Ventersdorp Contact Reef appear to be less bedded and substantially more siliceous than those present at Hartebeestfontein Mine. As a result of this greater strength, the rock in other mines would appear to be more susceptible to strain bursting under high stress conditions.

A typical time-dependent closure profile is given in Fig. 11. Evident is the high steady-state closure rate compared to that of the Ventersdorp Contact Reef, while the instantaneous closure at the time of blasting is small. A second data set is given

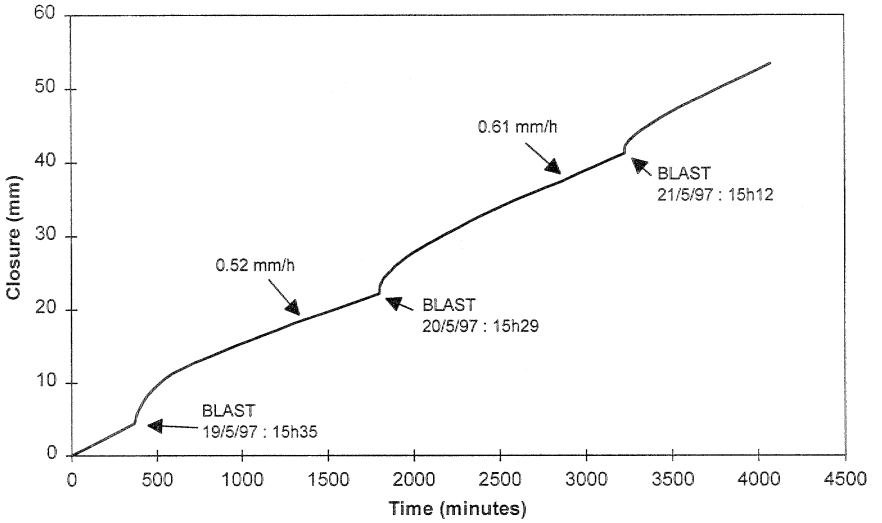

Fig. 11. Closure measured at Hartebeestfontein Mine. The instrument was 10.9 m from the face before the blast on 19/5/97. The steady-state closure rates were calculated for the periods from approximately 600 minutes after the blast until the next blast occurred

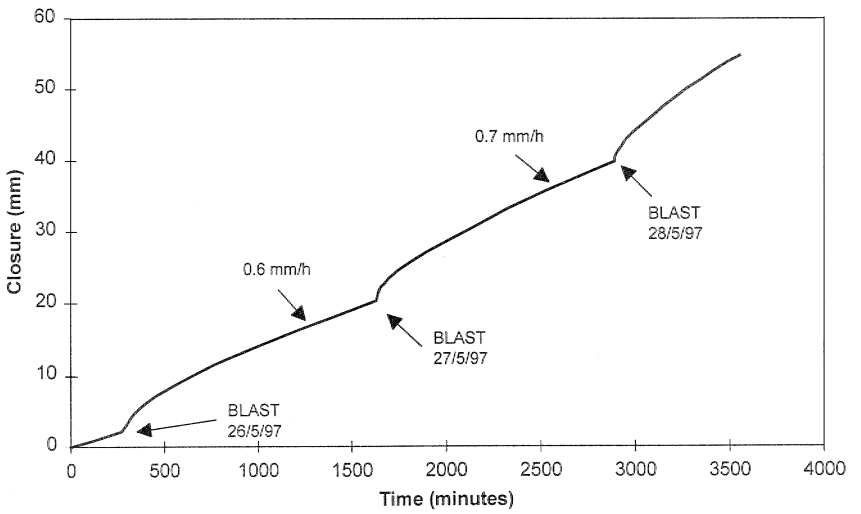

Fig. 12. Closure measurements at Hartebeestfontein Mine for a larger distance to face than that in Fig. 11. The instrument was 14.2 m from the face before the blast on 26/5/97

in Fig. 12. Note that the rate of steady-state closure increased as the instrument moved further away from the face. This is unlike measurements taken in the Ventersdorp Contact Reef stopes. A significant difference in the geotechnical properties of this area, compared to the Ventersdorp Contact Reef, is the presence of well-defined bedding planes. It appears that slip and dilation of these bedding

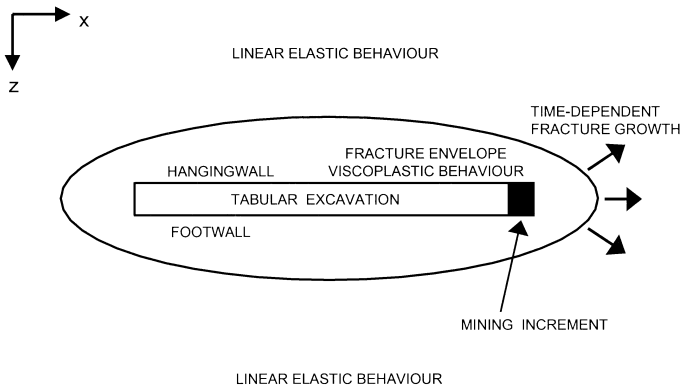

Fig. 13. Conceptualization of the fracture zone surrounding tabular excavations (section view) and time-dependent extension of this zone following a mining increment. The coordinate system is similar to that in Fig. 1, with the y-direction out of the plane of the page

planes is an important mechanism controlling the closure behaviour. This, coupled with the rapid deterioration of the hangingwall due to time-dependent fracture processes, may explain the increase in steady-state closure rates for larger distances from the face. Control of the hangingwall strata is difficult and these areas might be prone to falls of ground.

3. Modelling the Time-dependent Stope Behaviour

Linear viscoelastic theory is commonly used to simulate the time-dependent behaviour of rock. Although it is not possible to simulate rock failure and inelastic movements, even recent publications can be found where this theory is used (Pan and Dong, 1991; Yang et al., 1996). Malan (1998), however, found that there are some subtle problems associated with the use of viscoelastic theory to simulate the time-dependent behaviour of tabular excavations in hard rock. These problems arise from the special tabular geometry of the excavations and are not readily apparent when applying the theory to circular tunnels. From the discussion in Section 1, it is evident that the time-dependent failure processes in the rock play a prominent role in the time-dependent behaviour of these tabular excavations. It appears as if the significant time-dependent effects are confined to the fracture envelope surrounding the tabular excavations. The far field rock mass behaviour has been shown to be adequately represented by elastic theory (Ryder and Officer, 1964). An idealisation of this concept is given in Fig. 13. Note that the actual shape of the fracture envelope is not necessarily as depicted in the figure.

To include failure processes in rheological models, slider elements (also called St. Venant elements) are typically added to the elastic and viscous elements of viscoelasticity. These slider elements have a specified failure strength and are immobilised below this strength. Commonly, a viscous element is placed in parallel with the slider to control the strain rate if the slider is loaded above its failure strength. This is the so-called Bingham unit. Various combinations of elastic, vis-

cous and St. Venant elements have been used by researchers to simulate particular time-dependent problems. Gioda (1982) and Gioda and Cividini (1996) used a Kelvin viscoelastic model in series with a Bingham unit to represent primary and secondary closure in squeezing tunnels. Tertiary movements can be considered by providing suitable laws relating the values of the mechanical parameters (such as viscosity) to the irreversible part of the time-dependent strain. These rheological models are particularly suited for implementation in the finite element method. Other examples of the use of these rheological models can be found in Akagi et al. (1984), Song (1993), Lee et al. (1995), Euverte et al. (1994) and Sagawa et al. (1995).

Nawrocki (1995) developed a one-dimensional semi-analytical solution for the time-dependent behaviour of a coal seam. A Bingham type of material model was assumed. This study was initiated to investigate the rate of face advance on rockburst occurrence. The analysis showed that rapid ore extraction produces zones of high stress concentrations close to the longwall face. This situation is deemed to be hazardous as it increases the likelihood of rockbursting.

Since Perzyna (1966) proposed the general concept of elasto-viscoplasticity, a number of workers have applied this theory to geological materials. Elasto-viscoplasticity is essentially a modification of classical plasticity theory through the introduction of a time-rate rule in which the yield function and plastic potential function of classical plasticity are incorporated. In comparison with viscoelasticy, a viscoplastic material shows viscous behaviour in the plastic region only. Desai and Zhang (1987) used this theory together with a generalised yield function to characterise the viscoplastic behaviour of sand and rock salt. Sepehr and Stimpson (1988) used Perzyna's theory as a basis to develop a time-dependent finite element model to understand the time-dependent closure of excavations and seismicity in the potash mines in Saskatchewan. For a rheological analysis of tunnel excavations, Swoboda et al. (1987) developed a coupled finite element/boundary element approach to analyse the interaction of the rock with the viscoelastic properties of the shotcrete. The rock was assumed to behave in an elasto-viscoplastic fashion.

Fakhimi (1992) and Fakhimi and Fairhurst (1994) proposed a visco-elastoplastic constitutive model to simulate the time-dependent behaviour of rock. The model consists of an elasto-plastic Mohr-Coulomb model in series with a linear viscous unit. This model was implemented in an explicit finite difference code. A typical solution cycle would be to do an elasto-plastic analysis, during which real time is frozen. After an equilibrium point is reached, the linear viscous unit is used to determine additional creep strain components for a specified period of real time. Control is then passed back to the elasto-plastic analysis to obtain a new equilibrium and the process is repeated. Although this model appeared successful in imitating the behaviour of uniaxial and triaxial tests and the stand-up time of excavations, the time dependent behaviour of the model is independent of the failure processes. The entire material (including the far field) also behaves in a viscous manner. This model is therefore not applicable to the conceptual model of deep excavations in hard rock (Fig. 13), where the time-dependency is a direct consequence of the failure processes and the solid rock behaves essentially elastically.

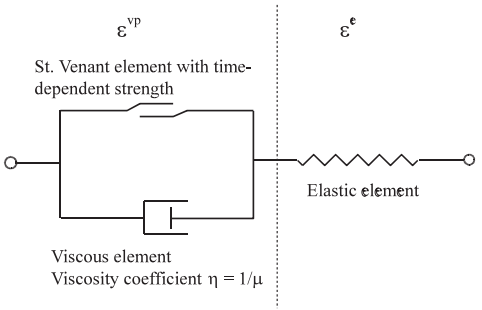

Fig. 14. Representation of the developed elasto-viscoplastic model

3.1 Elasto-Viscoplastic Formulation

For this study, classical elasto-viscoplasticity as defined by Perzyna (1966) is used as a basis for the formulation. Figure 14 shows the rheological analogue of the developed model. The strength of the slider is controlled by a novel time-dependent weakening rule as described below. Similarly to elasto-plastic theory, the concepts of yield function and flow rule also apply. However, in viscoplasticity theory, stresses above the yield surface are permissible.

Yield Surface

A time-dependent Mohr-Coulomb shear yield function is assumed and is given by

$$f_s(t) = \sigma_1 - \sigma_3 N_{\phi c} + 2C_c\sqrt{N_{\phi c}} \tag{1}$$

and

$$N_{\phi c} = \frac{1 + \sin\phi_c}{1 - \sin\phi_c}, \tag{2}$$

where ϕ_c is the current value of friction angle, C_c is the current value of cohesion, σ_1 is the major principle stress and $\sigma_1 < \sigma_2 < \sigma_3$ for a convention of negative compressive stresses. Equation (1) is a function of time t owing to a time-dependent reduction in the value of the cohesion C_c once the rock fails. This is explained below.

Shear failure takes place for $f_s(t) \leq 0$. For $f_s(t) > 0$, the rock behaves elastically. The cohesion C_c and friction angle ϕ_c will assume peak values C_p and ϕ_p for intact rock. Therefore the shear yield function $f_s(t)$ is not a function of time for intact rock. For intact rock, Eq. (2) becomes

$$N_{\phi p} = \frac{1 + \sin\phi_p}{1 - \sin\phi_p}. \tag{3}$$

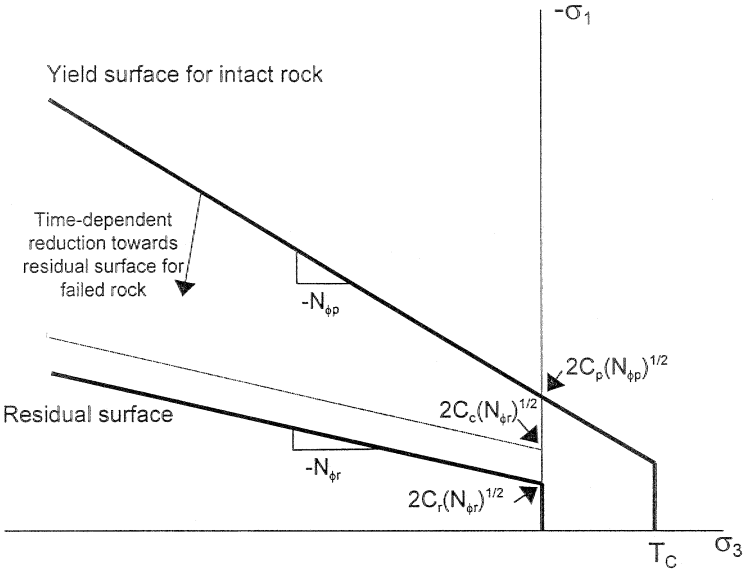

Fig. 15. The evolution of the yield surface for intact rock to the eventual residual surface for failed rock. Note that compressive stresses are negative and that on the vertical axis the negative of the major principal stress is plotted to turn the figure upright. $N_{\phi r}$ is defined in Eq. (10). T_C is the tensile strength of intact rock

Once the particular volume of rock starts failing, the friction angle assumes a residual value ϕ_r and the cohesion gradually decays to a residual value C_r. This cohesion softening process is simulated as a time-dependent process which is described later. This is also depicted in Fig. 15. It should be noted that the model can be easily extended to also allow for a time-dependent variation in the value of friction angle. For the modelling of non-linear rock failure behaviour, strain softening constitutive models are often used where both cohesion and friction varies with plastic strain (but not with time). The failure of Lac du Bonnet granite in laboratory compression tests (Martin, 1997) can be used as an example of the behaviour of hard rock. As the rock becomes damaged due to increasing strain, a portion of its cohesive strength is lost and friction is mobilized to its peak value. For small amounts of damage, the cohesion loss is rapid and can amount to 50% or more of the initial cohesion. The friction attains a peak value for small amounts of damage and then gradually decreases with increasing damage. From work done by Martin (1997) in the Underground Research Laboratory in Manitoba, Canada, it appears that at low confining stresses, such as those which occur in the near field rock mass around underground openings, the brittle-failure process in hard rock is dominated by cohesion loss. When developing the constitutive law in Eq. (1) for this current study, it was therefore assumed that the cohesion softening plays a dominant role in the time-dependent behaviour. For simplicity, the reduction in friction angle is assumed to be independent of time. For the numerical examples in Sections 3.2 and 4, this is irrelevant as it was assumed that $\phi_p = \phi_r$.

Flow Rule

If shear failure is detected, the viscoplastic strain rate $\dot{\varepsilon}_i^{vp}$ is given by

$$\dot{\varepsilon}_i^{vp} = \mu \langle f_s(t) \rangle \frac{\partial g_s}{\partial \sigma_i} \quad \text{for } i = 1, 2, 3 \tag{4}$$

where μ is the fluidity parameter and

$$\begin{aligned} \langle f_s(t) \rangle &= f_s(t) \quad \text{for } f_s(t) \leq 0 \\ \langle f_s(t) \rangle &= 0 \quad \text{for } f_s(t) > 0. \end{aligned} \tag{5}$$

A non-associated flow rule is used (Vermeer and De Borst, 1984) where the plastic potential function is given by

$$g_s = \sigma_1 - \sigma_3 N_\psi + 2C_c \sqrt{N_\psi} \tag{6}$$

with

$$N_\psi = \frac{1 + \sin \psi}{1 - \sin \psi} \tag{7}$$

and ψ is the dilation angle. From Eq. (4) it follows that in the model the strain rate of the failed rock is proportional to the excess stress above the yield surface.

Time-dependent Strength

A constitutive description of time-dependent rock behaviour should include the effect of strength degradation with time and/or deformation. Experimental evidence (Kranz et al., 1982) indicated that rock under load shows a decrease in strength with time. Fakhimi and Fairhurst (1994) modelled the time-dependent degradation of material strength by exponential friction and cohesion decay functions. Aydan et al. (1996) simulated the time-dependent behaviour of squeezing rocks as the degradation of strength properties as a function of time by utilising information obtained from creep tests.

Observations of time-dependent fracturing ahead of tabular stopes and in some haulages in the South African gold mines show that the rock becomes progressively more fractured with time, resulting in the gradual loss of cohesive strength in a particular volume of rock. This loss of strength will be modelled by assuming that the rate of cohesion reduction is proportional to the excess stress above the residual target surface (also see Eqs. (I.11) and (I.12) in Appendix I)

$$\dot{C}_c = k_c \langle f_{\text{res}} \rangle, \tag{8}$$

where k_c is the cohesion decay factor and

$$f_{\text{res}} = \sigma_1 - \sigma_3 N_{\phi r} + 2C_r \sqrt{N_{\phi r}} \tag{9}$$

$$N_{\phi r} = \frac{1 + \sin \phi_r}{1 - \sin \phi_r} \tag{10}$$

is the residual target surface. The principle embodied in Eq. (8) is based on laboratory observations (Malan, 1998) that if rock specimens are loaded close to the uniaxial strength, the creep rate and eventual creep failure occur faster than for a low stress. For a particular volume of rock under high stress, creep fractures will therefore form more rapidly, resulting in a faster loss of cohesion in the rock than for low stress.

The model developed above was implemented in a creep version of the computer program FLAC (Itasca, 1993) using the built-in FISH language. Any other suitable finite difference or finite element code could, however, be used. FLAC is an explicit finite difference code developed for geotechnical engineering applications. The two-dimensional version of the code was used in this study. FISH is a programming language embedded within FLAC, enabling the user to define new variables, functions and constitutive models. The creep version of FLAC gives access and control over a timestep that represents real time. Appendix I gives some detail regarding this implementation in FLAC.

3.2 Simulating the Closure Behaviour of Tabular Excavations

Malan and Bosman (1997) used the model described above to succesfully simulate the time-dependent increase in the extent of the fracture zone around squeezing tunnels. Soon after development of the tunnel, the failed zone covered those areas where the stresses exceeded the failure strength of the intact rock ($f_s(t) \leq 0$). Time-dependent processes lead to a gradual loss of residual strength in the fractured rock, transferring stress to the unfailed rock. This then also becomes fractured, resulting in a time-dependent increase in the extent of the fracture zone. Depending on the chosen model properties, an equilibrium position is eventually reached with no further growth in the fracture zone.

To investigate the applicability of the model for simulating time-dependent stope closure, the incremental mining of a panel was investigated. Figure 16 illustrates the geometry used. The size of the finite difference mesh was 100×80 elements, appropriately graded to ensure that the boundaries were sufficiently far away from the stope. The size of the elements in the area of the stope was 0.2 m, while the size of each mining increment was 1 m. Quarter symmetry was used to save on the number of elements. The stoping width was 1.2 m, although only 0.6 m is shown in Fig. 16 due to the imposed symmetry. Note the direction of the vertical (σ_v) and horizontal (σ_h) stress on the boundary of the model in Fig. 16. When applying the shear failure criteria in Eq. (1), the major (σ_1) and minor (σ_3) principal stresses need to be determined. The out-of-plane stress is taken as a principal stress with three different cases recognised. The out-of-plane stress is either (1) the major principal stress, (2) the minor principal stress or (3) the intermediate principal stress. The Cartesian stress components (horizontal, vertical and out-of-plane stresses) are resolved into principal stresses and ordered so that $\sigma_1 < \sigma_2 < \sigma_3$. The directions of the two in-plane principal stresses vary with position around the stope. Typical magnitudes and directions of these principal stresses around tabular stopes can be seen in Napier (1990). Although the model appeared successful in

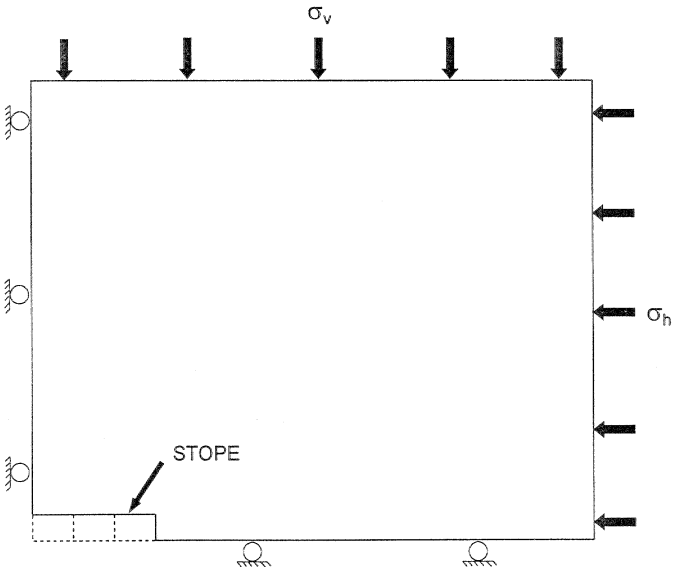

Fig. 16. Geometry and boundary conditions used for simulating tabular excavations (not drawn to scale)

replicating the closure behaviour as explained below, very large computer run-times were recorded. The explicit solution scheme of FLAC requires a small timestep to ensure stability. Following a large instantaneous stress change (for example after a mining increment), the timestep must be very small. Only as a new equilibrium state is approached, can the timestep be progressively enlarged. The run-time for ten mining increments in the simulation of Fig. 16 with weak rock properties can easily exceed 72 hours on a 200 MHz Pentium computer. This currently prohibits the simulation and calibration of incremental stope behaviour if the span is large. For the illustrative stope problems in Section 4, a low number of mining increments was used with high field stresses to obtain the required high stresses ahead of the face.

To investigate the simulated closure behaviour of a tabular excavation, eight increments were mined (giving a total span of 16 m), using the properties given in Table 2. Typical closure results are given in Fig. 17 as a function of time after mining the 8^{th} increment. For the two distances from the face, behaviour similar to that noted for the experimental results of the Ventersdorp Contact Reef is obtained. The incremental jump after blasting is reduced as the distance to face increases. Furthermore, the closure rate of the steady-state phase also decreases into the back area. These results are encouraging as this behaviour cannot be simulated with a viscoelastic model, as explained in Malan (1998). The visco-plastic model approximates the time-dependent failure processes and therefore gives the correct closure response for the Ventersdorp Contact Reef. No attempt was made to simulate the Vaal Reef as the behaviour of this reef is dominated by the bedding plane movements. The finite difference mesh is not suitable for the

Table 2. Properties used for the incremental mining of the tabular stope to obtain the results in Fig. 17

Parameter	Value
Vertical stress, σ_v	60 MPa
Horizontal stress, σ_h	30 MPa
Bulk modulus, K	38.9 GPa
Shear modulus, G	29.2 GPa
Density of the rock, ρ	2700 kg/m^3
Cohesion of intact rock, C_P	22 MPa
Friction angle (Both peak, ϕ_P, and residual, ϕ_R)	30°
Residual cohesion, C_r	10 MPa
Cohesion decay, k_C	0.005 h^{-1}
Dilation angle, ψ	0°
Fluidity coefficient, μ	1×10^{-10} Pa^{-1}.h^{-1}

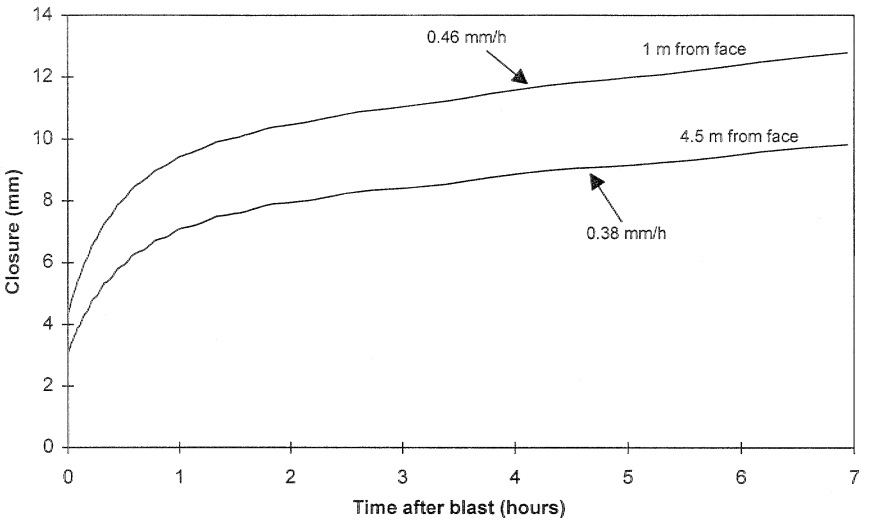

Fig. 17. Simulated time-dependent closure. The distances were the original distance to face before mining the increment. The steady-state closure rate was calculated between 2 hours and the end of the data set. Note that although only the first 7 hours after the mining increment is plotted, the time period between each step was 24 hours

inclusion of multiple discontinuities to simulate these parallel bedding planes. To simulate the time-dependent behaviour within an assembly of explicit discontinuities, Napier and Malan (1997) developed a discontinuum viscoplastic model suitable for implementation in a boundary element code.

In the example above, arbitrary model parameters were used to illustrate the closure profiles. Due to the success of this model in simulating the time-dependent fracture process, it is desirable to calibrate these parameters using underground closure data. The two-dimensional plain strain version of FLAC was used and therefore only geometries, where these assumptions can be made, are appropriate. As the results obtained from viscoplasticity theory are path dependent, the entire

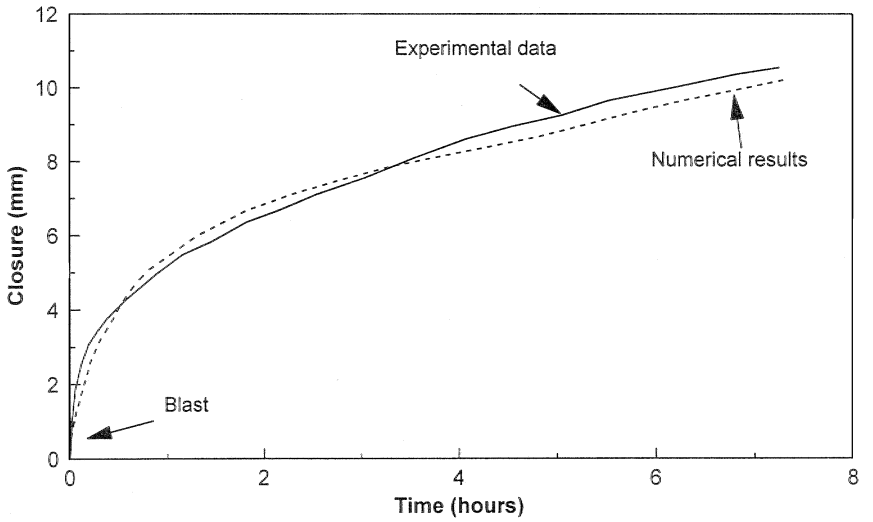

Fig. 18. Experimental and simulated stope closure after blasting

stope span cannot be simulated in one mining increment. Data was therefore needed where the span of the stope was small. Closure data collected by Kersten (1995) at Hartebeestfontein Mine in 1965 was used. The geometry was such that a two-dimensional plane strain approximation could be made. The instrumented panel was situated at a depth of 1850 m, with a span of 20 m. The actual stress conditions and rock parameters are not known accurately and therefore the objective of this simulation was not exact parameter calibration, but an attempt to replicate the observed profiles. The closure fitting process was very arduous as ten mining increments (using symmetry) had to be mined. It was found that the path dependence and slow run times made it very difficult to achieve the desired final closure by making small changes in the parameter values before the first increment. In spite of these problems, it should be noted that the closure behaviour of the viscoplastic model gives similar trends to that of the underground measurements. Figure 18 shows the experimental data and numerical results for a fluidity coefficient of $1 \times 10^{-10}\,\mathrm{Pa^{-1}h^{-1}}$ and a cohesion decay rate of $0.005\,\mathrm{h^{-1}}$. Other parameters used were bulk modulus = 38.8 GPa, shear modulus = 29 GPa, cohesion = 22 MPa, residual cohesion = 15 MPa and friction angle (peak and residual) = 30°. In the model, the stope was mined incrementally to the required span, using 1 m increments.

4. The Use of Closure Data as a Diagnostic Measure of Rock Mass Behaviour

When comparing typical results of the Vaal Reef in Fig. 11 with those of the Ventersdorp Contact Reef in Fig. 5, it is clear that significant differences exist between the continuous closure profiles of these different geotechnical areas. For a more direct comparison, typical closure increments after blasts for these two areas

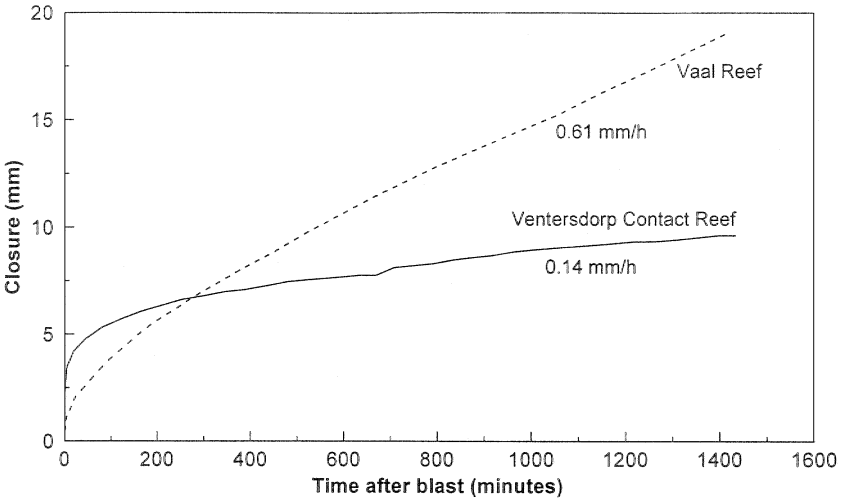

Fig. 19. Comparison of typical closure profiles of the Ventersdorp Contact Reef (hard lava) and Vaal Reef. For the Vaal Reef measurements the instrument was 11.5 m from the face before the blast while it was 10 m from the face for the Ventersdorp Contact Reef measurements

are plotted in Fig. 19. The two experimental sites are approximately at the same depth and, for these specific data sets, the closure instruments were approximately the same distance from the face. Although care should be taken when comparing these sites directly, owing to different mining geometries, the following important differences are noted. The closure behaviour of the Ventersdorp Contact Reef (hard lava) is characterised by a large instantaneous jump after blasting followed by a low closure rate. These areas appear to be prone to face bursting. In contrast, for the Vaal Reef, the closure is characterised by a small instantaneous jump after blasting followed by a high rate of closure. The risk of face bursting is low in these areas, although the risk of falls of ground is more pronounced.

The instantaneous jump in closure after blasting is the result of the immediate redistribution of stress following the removal of an increment of rock in the face. The more significant the disturbance to the stress field, the more pronounced the immediate response will be. If the increment of rock removed by blasting carries no load (in essence loose rock lying at the face) no change in the stress field will take place and no change will be noticed in the closure behaviour. The instantaneous closure response after blasting therefore appears to indicate the role the removed rock played in maintaining the stress equilibrium before the blast. For the Ventersdorp Contact Reef, the significant instantaneous closure after blasting is probably an indicator of a more highly stressed face area than the Vaal Reef. This may explain why face bursting appears to be more pronounced on this reef than the Vaal Reef.

A further difference in behaviour between these areas is the high rate of steady-state closure of the Vaal Reef stopes compared to the Ventersdorp Contact Reef (hard lava) stopes. The high steady-state closure rate is an indication of efficient stress redistribution through mobilization and growth of the fracture zone and slip

Table 3. Parameters used in the simulation to obtain the results in Fig. 20 and Fig. 21. As the stope span was small in this simulation, large stresses and weak rock properties were used to ensure a representative fracture zone ahead of the face

Parameter	Value
Vertical stress, σ_v	110 MPa
Horizontal stress, σ_h	55 MPa
Bulk modulus, K	38.9 GPa
Shear modulus, G	29.2 GPa
Density, ρ	2700 kg/m^3
Cohesion of intact rock, C_P	10 MPa
Friction angle (Both peak, ϕ_P, and residual, ϕ_R)	30°
Residual cohesion, C_r	3 MPa
Cohesion decay, k_C	Stope A: 1×10^{-10} h^{-1} Stope B: 0.01 h^{-1}
Dilation angle, ψ	15°
Fluidity coefficient, μ	1×10^{-10} Pa^{-1}.h^{-1}

on discontinuities, such as bedding planes. This in turn may result in low face stresses. Although the face bursting hazard might be low in areas with high steady-state closure rates, the large time-dependent behaviour of the fracture zone might lead to a rapid deterioration of hangingwall, thereby increasing the fall of ground hazard.

It was suggested above that the instantaneous closure after blasting is an indication of the proximity of the stress peak to the face. This hypothesis was tested by simulating two stopes (A and B), using the viscoplastic model described above. The parameters used are given in Table 3. The only difference between these stopes is a different rate of cohesion decay. This resulted in the rock ahead of the face of Stope B losing its strength much faster than the rock ahead of Stope A, therefore carrying less load. This is illustrated in Fig. 20, where the major principle stress is plotted against distance ahead of the original face position just before an increment is mined. Visible in this figure is the stress peak for both stopes some distance ahead of the face. With sufficient distance from the face, the stress magnitude is reduced to the virgin value. For Stope A the peak is closer to the face. The next increment of mining will remove the first metre of rock thereby forcing the stress carried by this increment to be instantaneously redistributed. As the average stress in this increment of rock is larger for Stope A than Stope B, it is expected that the instantaneous closure will be bigger for A. This is confirmed by the closure that followed this increment in Fig. 21. For Stope A the instantaneous closure was 3.7 mm, compared to the 2.5 mm for Stope B. Following the instantaneous closure, the steady-state closure for Stope B is larger as the failed rock loses its strength faster, resulting in greater time-dependent deformation.

Figure 20 illustrates the position of the peak stress 24 hours after mining an increment. This position is not stationary but moves as the time-dependent fracture processes occur in the rock. To illustrate this, Fig. 22 illustrates the stress peak for various times after mining the particular increment of Stope B. Soon after the blast the peak is high and located close to the face. With time it moves away, due to the fracture processes, gradually becoming smaller. Of significance is that the

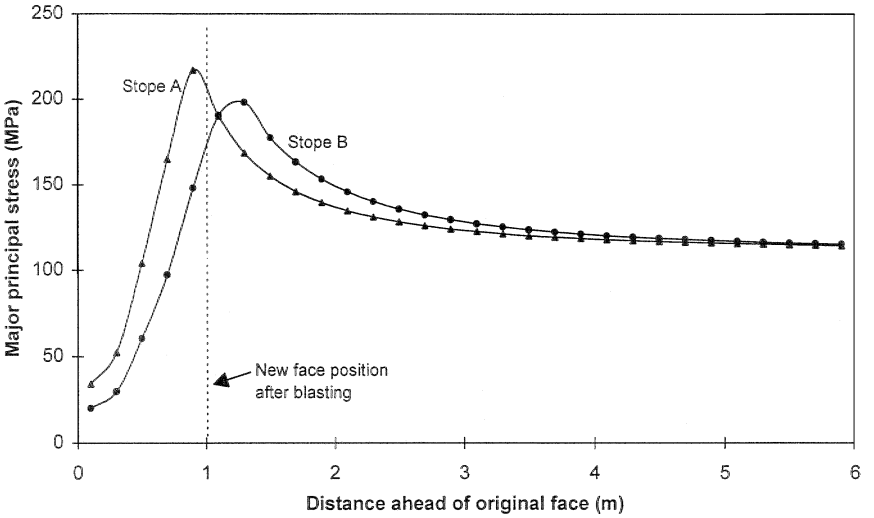

Fig. 20. Major principal stress as a function of distance ahead of the face for the two simulated stopes. These stresses were calculated in the centre of the reef

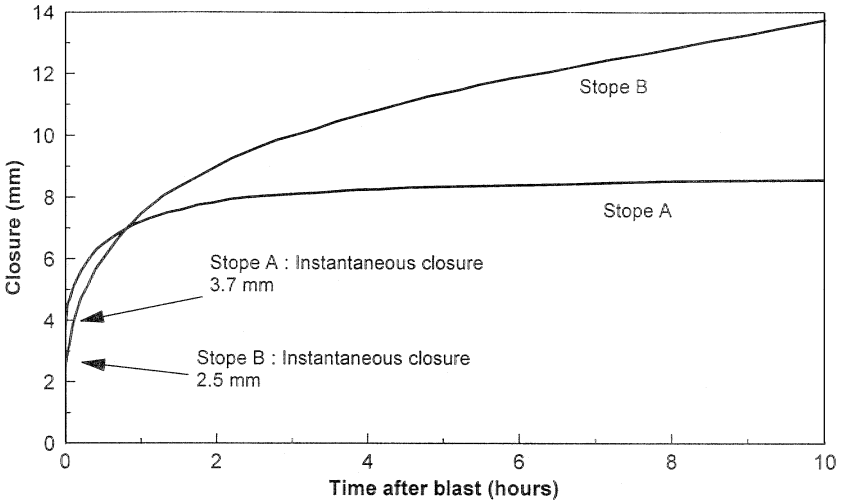

Fig. 21. Comparison of the simulated closure behaviour as a function of time after the blast. The measurement position was 0.5 m behind the original face

biggest stress change happens within the first five hours. This is also the approximate duration of the primary closure phase for stope B in Fig. 21.

It appears then that the instantaneous closure observed underground might be used as an indication of the stress magnitude in the face area and, therefore, also an indicator of the face bursting hazard. It should, however, be emphasised that the instantaneous closure response after a blast is a reflection of the face stress

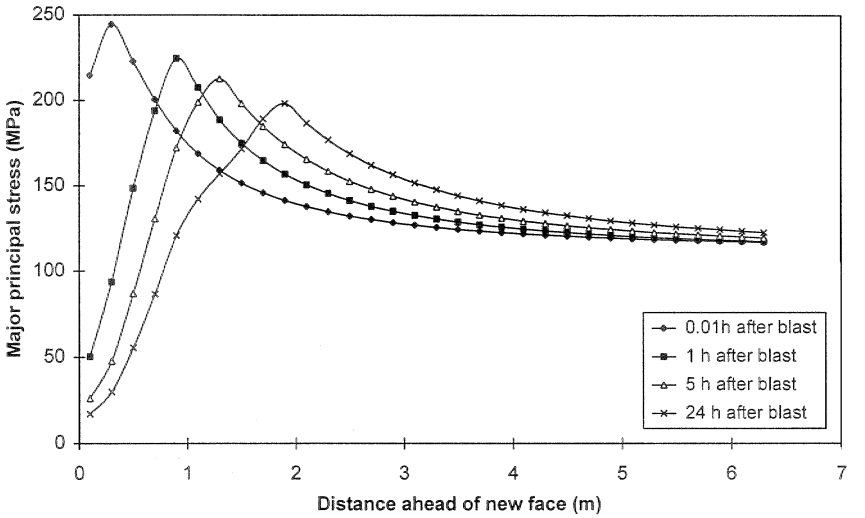

Fig. 22. Simulated time-dependent movement of the major principal stress peak ahead of the face after blasting due to the migration of the fracture zone

before the blast and not after it. Underground measurements (Fig. 25) indicate that the instantaneous closure appears to include a random component and is therefore not deterministic. This random component might be caused by the varying rock properties (and therefore varying stress magnitudes) ahead of the face, although mining technique and measurement position also play a strong role. If only a portion of the face is blasted and not the entire length, the instantaneous closure at a particular measurement position will be smaller. The uninformed observer might then be deceived into concluding that the face stress is dropping. Due to these factors, prediction of face bursting would be very difficult if not impossible. The value of these closure measurements should rather be seen as the possible identification of hazardous areas. An average value of instantaneous closure taken over a specified period might be useful to define a face bursting risk. This can be seen from the data collected underground where the average instantaneous closure of the Ventersdorp Contact Reef (hard lava) is clearly much higher than that of the Vaal Reef.

4.1 The Effect of Preconditioning on Time-dependent Closure Behaviour

Preconditioning is a technique used in the South African gold mining industry to "engineer" the fracture zone ahead of advancing mining faces. Large stresses are occasionally present in the fracture zone close to the face because of interlocking discontinuities or low fracture densities. This can result in sudden stress release through face bursting. Preconditioning is used in these areas to help sustain the normal development of the fracture zone and push the stress peak further ahead of the face. The technique consists of drilling long holes, either parallel or perpen-

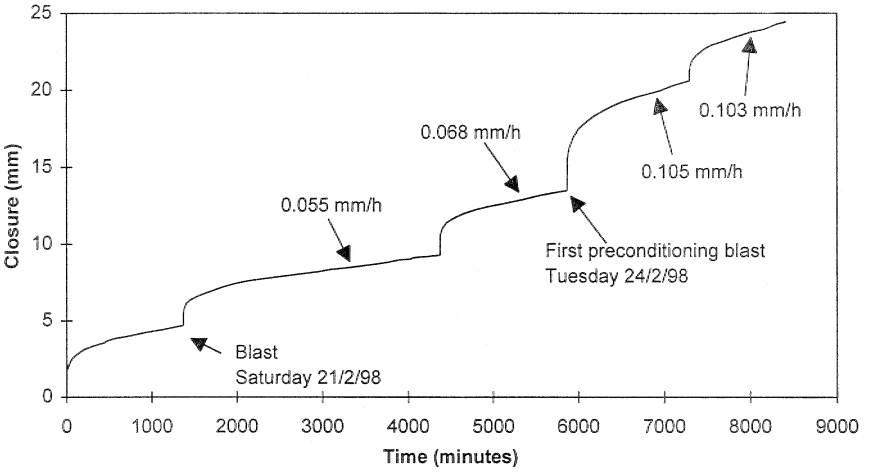

Fig. 23. The effect of preconditioning on the time-dependent closure of a stope in the Ventersdorp Contact Reef. The values indicated in the figure are the steady-state closure rates and were calculated for the periods of 800 minutes after the blast until the next blast occurred. The instrument was 7.2 m from the face at the beginning of this data set and 10.5 m from the face after the last blast in the figure

dicular to the face. The perpendicular holes (used at Western Deep Levels Mine) are typically 2.4 m deep and are blasted as part of the production sequence. Kullmann et al. (1996) reported that these preconditioning blasts did indeed achieve the desired objectives.

Preconditioning was not used in the stopes described in Section 2 of this paper. The closure data presented therefore does not include the effect of preconditioning. Since collection of this data, preconditioning was introduced in the 87-49 longwall at Western Deep Levels Mine. Measurements were taken in a panel not far from those depicted in Fig. 4. Typical results are illustrated in Fig. 23. Note that the steady-state closure rate increases significantly after the onset of preconditioning. This is further illustrated in Fig. 24, which compares the rate of steady state closure as a function of distance from the face for panels with and without preconditioning. These rates were calculated for 10 hours to approximately 24 hours after each blast. It is clear from this that the steady-state creep rate is significantly increased with preconditioning. This is probably an indication of enhanced time-dependent deformation of the rock mass that reduces the amount of strain energy stored close to the face and therefore also the likelihood of face bursting.

It is not clear at this stage what the effect of preconditioning is on the instantaneous closure response after blasting. In Fig. 23, the instantaneous response after the first preconditioning blast was significantly higher than the previous blasts. This might be the result of the 2.4 m deep preconditioning blasts affecting a larger volume of stressed rock, compared to ordinary production blasting. Figure 25 compares the instantaneous closure after blasting with and without preconditioning. Note that there is not a distinct difference for the two cases, although the values for the preconditioning appear to be slightly higher. Also note that there appears to be a poor correlation between magnitude of instantaneous closure and

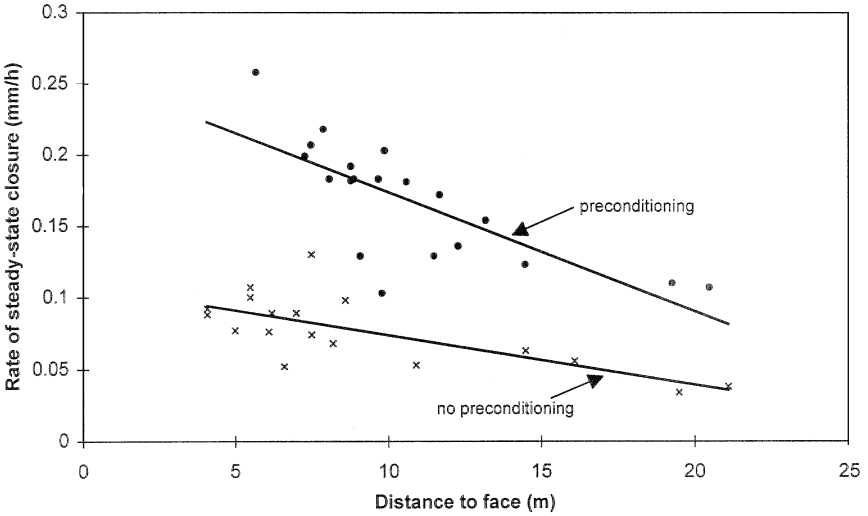

Fig. 24. The effect of preconditioning on the rate of steady-state closure for panels in the Ventersdorp Contact Reef

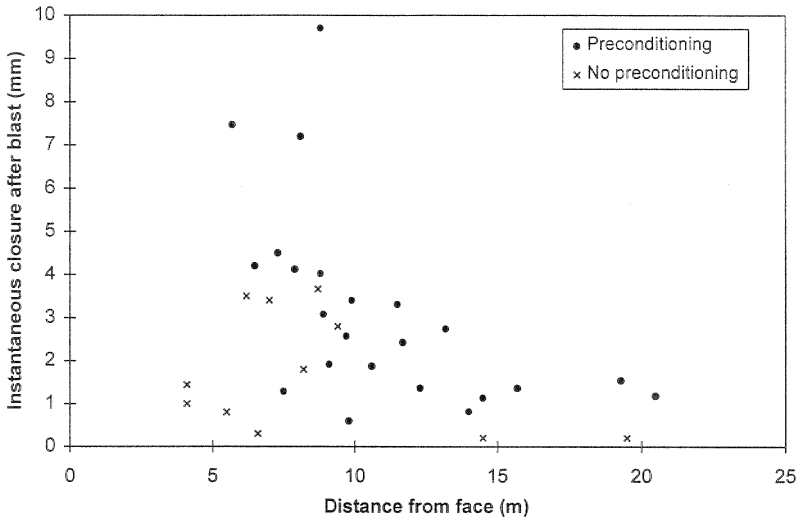

Fig. 25. The effect of preconditioning on the instantaneous closure after blasting of the Ventersdorp Contact Reef

distance to face. One factor causing this is the position of the closure instrument in the direction parallel to the face. This geometrical effect is illustrated in Fig. 8. The length of face advance for the particular blast and whether the entire face or only a portion is blasted, also plays a role. For a fixed position in the direction parallel to the face, it is found that the instantaneous closure typically reduces in magnitude as the distance to the face, increases. This can be seen in Fig. 6 and Fig. 7.

5. Conclusions

Although excavations in hard rock are not usually perceived to undergo significant time-dependent deformation owing to the low creep rate of intact rock, data from the deep gold mines in South Africa illustrates behaviour to the contrary. Closure measurements in the tabular excavations indicate significant time-dependent deformation. Although the excavations are developed in brittle quartzite and lava, the rate of steady-state closure can be as high as 0.7 mm/h in certain areas. The closure behaviour of these excavations typically consists of an instantaneous response at blasting time, followed by a primary phase of decelerating closure, lasting approximately five hours, and a steady-state closure phase. This pattern is repeated after the next blast. This time-dependent closure behaviour is the result of the rheological behaviour of the fracture zone that surrounds these excavations. After a mining increment, the fracture zone extends in a time-dependent fashion ahead of the working faces. The majority of new fractures appear to form within approximately the first five hours after the blast. Thereafter, the number of new fractures decreases until the next blast occurs.

For tabular excavations in the Ventersdorp Contact Reef (hard lava), the instantaneous closure response is very prominent, but decreases in magnitude as the distance from the face to the measurement position increases. The steady-state closure rate also decreases in magnitude with distance to the face. In contrast, for excavations in certain areas of the Vaal Reef, the steady-state closure rate can be as high as 15 mm/day. For these excavations the instantaneous closure response at blasting time is virtually absent. Unlike the Ventersdorp Contact Reef, the steady-state closure rate of the experimental panel in the Vaal Reef increases with increasing distance to the face. This difference in behaviour is caused by the presence of prominent bedding planes in the hangingwall of the Vaal Reef.

To allow for direct simulation of the time-dependent fracture zone behaviour, a continuum viscoplastic model was developed. The model is based on classical viscoplasticity, with a novel time-dependent cohesion weakening rule to simulate the time-dependent failure of the rock. A Mohr-Coulomb failure law and a non-associated flow-rule were assumed. For an excavation in this material, the failure zone, soon after development, covers those areas where the stress exceeded the failure strength of the rock. The time-dependent processes lead to a gradual transfer of stress to the unfailed rock. This also becomes fractured, leading to a time-dependent growth of the fracture zone. The process continues until an equilibrium position is attained. This model has proved to be successful in simulating the time-dependent closure behaviour of tabular excavations, giving both the instantaneous response at blasting time and the primary and steady-state closure phases.

An important finding of this study is that the time-dependent closure data can possibly be used to deduce important information about the behaviour of the rock mass and the stress in the fracture zone ahead of the face. Although estimation of absolute stresses may not be feasible, the closure may be used to identify areas with large average face stresses and therefore an increase in the risk of face bursting. It appears that the instantaneous closure response at blasting time gives an

indication of the magnitude of stress in the face area. The larger the stress, the bigger the instantaneous closure response following the mining increment. This hypothesis was successfully tested by simulating two stopes with different rock conditions using the continuum viscoplastic approach developed in this study. Some confirmation of the possible use of time-dependent closure data to determine a face burst hazard was obtained from the underground data. The Ventersdorp Contact Reef (hard lava) stopes appear to be prone to face bursting and, as mentioned above, the closure behaviour of these excavations typically includes a large instantaneous response after blasting. In comparison, in some areas of the Vaal Reef with a lower risk of face bursting, the instantaneous closure response after blasting is small. This important concept of using closure data as a diagnostic measure of face stress and as a hazard indicator is currently being investigated further.

Acknowledgements

This work forms part of the rockmass behaviour research programme of Rock Engineering, CSIR Division of Mining Technology. The financial assistance and support received from the Safety in Mines Research Advisory Committee (SIMRAC) is acknowledged. The author recently completed a Ph.D degree at the University of the Witwatersrand and the work described here also formed part of that study. The personnel of the Rock Mechanics Departments at Hartebeestfontein Mine and Western Deep Levels Mine, South Shaft, are thanked for their assistance in providing panels for the experimental closure measurements. Dr. John Napier, Mr. Van Zyl Brink and Mr. Mike Roberts reviewed the manuscript and improved the quality of the work with their helpful comments.

Appendix I. Implementation of the Elasto-Viscoplastic Model in FLAC

When a new constitutive model is written for FLAC, using the built-in language FISH, the main task is to update the stress tensor in each timestep for the given old stress tensor and strain components at the start of the timestep (Itasca, 1993). For the viscoplastic model developed in Section 3, the rock behaves elastically if the failure strength is not exceeded. During each cycle in the program stepping, each element is tested for failure using Eq. (1). For elements that have not failed, $C_c = C_p$ and $\phi_c = \phi_p$. Once the element fails, ϕ_c is set to ϕ_r while C_c is gradually reduced from C_p to C_r as explained below.

For elements where the stress exceeds the failure strength, the total strain increment is given by

$$\Delta\varepsilon_i = \Delta\varepsilon_i^e + \Delta\varepsilon_i^{vp} \quad \text{for } i = 1, 2, 3. \tag{I.1}$$

Writing Eq. (4) in incremental form gives

$$\Delta\varepsilon_i^{vp} = \mu\Delta t\langle f_s(t)\rangle \frac{\partial g_s}{\partial \sigma_i} \quad \text{for } i = 1, 2, 3, \tag{I.2}$$

where Δt is the timestep. Inserting Eq. (6) in Eq. (I.2) and then in Eq. (I.1) gives

$$\begin{aligned}\Delta\varepsilon_1 &= \Delta\varepsilon_1^e + \mu\Delta t\langle f_s(t)\rangle,\\ \Delta\varepsilon_2 &= \Delta\varepsilon_2^e,\\ \Delta\varepsilon_3 &= \Delta\varepsilon_3^e - \mu\Delta t\langle f_s(t)\rangle N_\psi.\end{aligned} \tag{I.3}$$

The stress increments $\sigma_i' - \sigma_i^0$ are related to the elastic strain increments by the elasticity equations

$$\begin{aligned}\sigma_1' &= \sigma_1^0 + A\Delta\varepsilon_1^e + B(\Delta\varepsilon_2^e + \Delta\varepsilon_3^e),\\ \sigma_2' &= \sigma_2^0 + A\Delta\varepsilon_2^e + B(\Delta\varepsilon_1^e + \Delta\varepsilon_3^e),\\ \sigma_3' &= \sigma_3^0 + A\Delta\varepsilon_3^e + B(\Delta\varepsilon_1^e + \Delta\varepsilon_2^e),\end{aligned} \tag{I.4}$$

where

$$A = K + \frac{4G}{3}, \tag{I.5}$$

$$B = K - \frac{2G}{3}. \tag{I.6}$$

K is the bulk modulus and G the shear modulus of the rock. The initial estimate of new stresses (before testing for failure) is also derived from the elasticity relations

$$\begin{aligned}\sigma_1^I &= \sigma_1^0 + A\Delta\varepsilon_1 + B(\Delta\varepsilon_2 + \Delta\varepsilon_3),\\ \sigma_2^I &= \sigma_2^0 + A\Delta\varepsilon_2 + B(\Delta\varepsilon_1 + \Delta\varepsilon_3),\\ \sigma_3^I &= \sigma_3^0 + A\Delta\varepsilon_3 + B(\Delta\varepsilon_1 + \Delta\varepsilon_2).\end{aligned} \tag{I.7}$$

This can be written as

$$\begin{aligned}\sigma_1^0 &= \sigma_1^I - A\Delta\varepsilon_1 - B(\Delta\varepsilon_2 + \Delta\varepsilon_3),\\ \sigma_2^0 &= \sigma_2^I - A\Delta\varepsilon_2 - B(\Delta\varepsilon_1 + \Delta\varepsilon_3),\\ \sigma_3^0 &= \sigma_3^I - A\Delta\varepsilon_3 - B(\Delta\varepsilon_1 + \Delta\varepsilon_2).\end{aligned} \tag{I.8}$$

When inserting Eq. (I.3) this gives

$$\begin{aligned}\sigma_1^0 &= \sigma_1^I - A[\Delta\varepsilon_1^e + \mu\Delta t\langle f_s(t)\rangle] - B[\Delta\varepsilon_2^e + \Delta\varepsilon_3^e - \mu\Delta t\langle f_s(t)\rangle N_\psi],\\ \sigma_2^0 &= \sigma_2^I - A\Delta\varepsilon_2^e - B[\Delta\varepsilon_1^e + \Delta\varepsilon_3^e + \mu\Delta t\langle f_s(t)\rangle(1 - N_\psi)],\\ \sigma_3^0 &= \sigma_3^I - A[\Delta\varepsilon_3^e - \mu\Delta t\langle f_s(t)\rangle N_\psi] - B[\Delta\varepsilon_1^e + \Delta\varepsilon_2^e + \mu\Delta t\langle f_s(t)\rangle].\end{aligned} \tag{I.9}$$

This in turn can be inserted in Eq. (I.4) to give

$$\begin{aligned}\sigma_1' &= \sigma_1^I - \mu\Delta t\langle f_s(t)\rangle[A - BN_\psi],\\ \sigma_2' &= \sigma_2^I - B\mu\Delta t\langle f_s(t)\rangle[1 - N_\psi],\\ \sigma_3' &= \sigma_3^I - \mu\Delta t\langle f_s(t)\rangle[B - AN_\psi].\end{aligned} \tag{I.10}$$

Writing Eq. (8) in incremental format

$$\Delta C_c = k_c \langle f_{res} \rangle \Delta t. \tag{I.11}$$

At timestep $(j+1)$ the value of cohesion is given by

$$\begin{aligned} C_c^{j+1} &= C_c^j - \Delta C_c \quad \text{if } C_c^{j+1} > C_r, \\ C_c^{j+1} &= C_r \quad \text{if } C_c^{j+1} \leq C_r. \end{aligned} \tag{I.12}$$

The implementation of this model in FISH language can be found in Malan (1998).

References

Adams, G. R., Jager, A. J. (1980): Petroscopic observations of rock fracturing ahead of stope faces in deep-level gold mines. J. S. Afr. Inst. Min. Metall. 44, 204–209.

Adams, G. R., Jager, A. J., Roering, C. (1981): Investigations of rock fracture around deep level gold mine stopes. In: Einstein, H. H. (ed.) Proc., 22nd U.S. Symp. Rock Mech., 213–218.

Akagi, T., Ichikawa, Y., Kuroda, H., Kawamoto, T. (1984): A non-linear rheological analysis of deeply located tunnels. Int. J. Num. Anal. Meth. Geomech. 8, 457–471.

Aydan, Ö., Akagi, T., Kawamoto, T. (1996): The squeezing potential of rock around tunnels: Theory and prediction with examples taken from Japan. Rock Mech. Rock Engng. 29, 125–143.

Cook, N. G. W., Hoek, E., Pretorius, J. P. G., Ortlepp, W. D., Salamon, M. D. G. (1966): Rock mechanics applied to the study of rockbursts. J. S. Afr. Inst. Min. Metall. 66, 435–528.

Denkhaus, H. G., Hill, F. G., Roux, A. J. A. (1958): A review of recent research into rockbursts and strata movement in deep-level mining in South Africa. Ass. Min. Mngrs. S. Afr., 245–268.

Desai, C. S., Zhang, D. (1987): Viscoplastic model for geologic materials with generalised flow rule. Int. J. Num. Anal. Meth. Geomech. 11, 603–620.

Dusseault, M. B., Fordham, C. J. (1993): Time-dependent behavior of rocks. In: Hudson, J. A. (ed.) Comprehensive rock engineering, vol. 3. Pergamon Press Oxford, 119–149.

Euverte, C., Allemandou, X., Dusseault, M. B. (1994): Simulation of openings in visco-elastoplastic media using a discrete element method. In: Siriwardane and Zaman (eds.), Computer methods and advances in geomechanics. Balkema, Rotterdam, 809–814.

Fakhimi, A. A. (1992): The influence of time-dependent deformation of rock on the stability of underground excavations. PhD thesis, University of Minnesota.

Fakhimi, A. A., Fairhurst, C. (1994): A model for the time-dependent behavior of rock. Int. J. Rock Mech. Min. Sci. 31, 117–126.

Gay, N. C., Jager, A. J. (1980): The influence of geological features on rock mechanics problems in Witwatersrand gold mines. Chamber of Mines of South Africa, unpublished Research Report.

Gioda, G. (1982): On the non-linear "squeezing" effects around circular tunnels. Int. J. Num. Anal. Meth. Geomech. 6, 21–46.

Gioda, G., Cividini, A. (1996): Numerical methods for the analysis of tunnel performance in squeezing rocks. Rock Mech. Rock Engng. 29, 171–193.

Güler, G. (1997): Analysis of the rock mass behaviour as associated with Ventersdorp Contact Reef stopes, South Africa. M. Sc dissertation, University of the Witwatersrand, Johannesburg.

Gürtunca R. G. (1989): Results of a classified tailings monitoring programme at Vaal Reefs. COMRO (now CSIR Miningtek) Internal Report, no. 614.

Hodgson, K. (1967): The behaviour of the failed zone ahead of a face, as indicated by continuous seismic and convergence measurements, Chamber of Mines Research Report 31/61, Transvaal and Orange Free State Chamber of Mines Research Organisation.

Itasca (1993): FLAC – Fast Lagrangian Analysis of Continua: User's Manual.

Johnson, R. A., Schweitzer, J. K. (1996): Mining at ultra-depth: Evaluation of alternatives. In: Aubertin, M. Hassani, F., Mitri, H. (eds.) Proc., 2nd North Am. Rock Mech. Symp: NARMS '96, Montreal, 359–366.

Kersten, R. W. O. (1995): Personal communication.

King, R. G., Jager, A. J., Roberts, M. K. C., Turner, P. A. (1989): Rock mechanics aspects of stoping without back-area support. COMRO (Now CSIR Miningtek) Research Report, no. 17/89.

Kranz, R. L., Harris, W. J., Carter, N. L. (1982): Static fatigue of granite at 200 °C. Geophys. Res. Lett. 9, 1–4.

Kullmann, D. H., Stewart, R. D., Grodner, M. (1996): A pillar preconditioning experiment on a deep-level South African gold mine. In: Aubertin, M., Hassani, F., Mitri, H. (eds.) Proc., 2nd North Am. Rock Mech. Symp: NARMS '96, Montreal, 375–380.

Lee, C., Lee, Y., Cho, T. (1995): Numerical simulation for the underground excavation-support sequence in the visco-plastic jointed rock mass. In: Fujii, T. (ed.), Proc., 8th Int. Cong. Rock Mech., ISRM, Balkema, Rotterdam, 619–621.

Legge, N. B. (1984): Rock deformation in the vicinity of deep gold mine longwall stopes and its relation to fracture. Ph.D thesis, University College, Cardiff.

Linkov, A. M. (1996): Rockbursts and the instability of rock masses – Schlumberger Award Lecture. Int. J. Rock Mech. Min. Sci. Geomech Abstr. 33, 727–732.

Malan, D. F. (1998): An investigation into the identification and modelling of time-dependent behaviour of deep level excavations in hard rock. PhD thesis, University of the Witwatersrand, Johannesburg, South Africa.

Malan, D. F., Bosman, J. D. (1997): A viscoplastic approach to the modelling of time-dependent rock behaviour at Hartebeestfontein Gold Mine. In: Gürtunca R. G., Hagan, T. O. (eds.), SARES97, Johannesburg, 117–130.

Martin, C. D. (1997): Seventeenth Canadian Geotechnical Colloquium: The effect of cohesion loss and stress path on brittle rock strength. Can. Geotech. J. 34, 698–725.

Napier, J. A. L. (1990): Modelling of fracturing near deep level gold mine excavations using a displacement discontinuity approach. In: Rossmanith, H. P. (ed.), Proc., Mechanics of jointed and faulted rock. Balkema, Rotterdam, 709–715.

Napier, J. A. L., Malan, D. F. (1997): A viscoplastic discontinuum model of time-dependent fracture and seismicity effects in brittle rock. Int. J. Rock Mech. Min. Sci. Geomech. Abstr. 34, 1075–1089.

Nawrocki, P. A. (1995): One-dimensional semi-analytical solution for time-dependent behaviour of a seam. Int. J. Num. Anal. Meth. Geomech. 19, 59–74.

Pan, Y. W., Dong, J. J. (1991): Time-dependent tunnel convergence – I. Formulation of the model. Int. J. Rock Mech. Min. Sci. 28, 469–475.

Panet, M. (1996): Two case histories of tunnels through squeezing rocks. Rock Mech. Rock Engng. 29, 155–164.

Perzyna, P. (1966): Fundamental problems in viscoplasticity. Adv. Appl. Mech. 9, 243–377.

Roux, A. J. A., Denkhaus, H. G. (1954): An investigation into the problem of rockbursts – An operational research project. J. Chem. Metall. Min. Soc. S. Afr. 55, 103–124.

Ryder, J. A., Officer, N. C. (1964): An elastic analysis of strata movement observed in the vicinity of inclined excavations. J. S. Afr. Inst. Min. Metall. 64, 219.

Sagawa, Y., Yamatomi, J., Mogi, G. (1995): A rheology model for non-linear and time-dependent behaviour of rocks. In: Fujii, T. (ed.), Proc., 8th Int. Cong. Rock Mech. ISRM, Balkema, Rotterdam, 311–314.

Salamon, M. D. G., Ryder, J. A., Ortlepp, W. D. (1964): An analogue solution for determining the elastic response of strata surrounding tabular mining excavations. J. S. Afr. Inst. Mining Metall. 64, 115–137.

Schweitzer, J. K., Johnson, R. A. (1997): Geotechnical classification of deep and ultra-deep Witwatersrand mining areas, South Africa. Mineralium Deposita 32, 335–348.

Sepehr, K., Stimpson, B. (1988): Potash mining and seismicity: A time-dependent finite element model. Int. J. Rock Mech. Min. Sci. Geomech. Abstr. 25, 383–392.

Song, D. (1993): Non-linear viscoplastic creep of rock surrounding an underground excavation. Int. J. Rock Mech. Min. Sci. Geomech. Abstr. 30, 653–658.

Swoboda, G., Mertz, W., Beer, G. (1987): Rheological analysis of tunnel excavations by means of coupled finite element (FEM)-boundary element (BEM) analysis. Int. J. Num. Anal. Meth. Geomech. 11, 115–129.

Turner, P. A. (1984): Report on an investigation of several hard patches in the mechanical mining site at Doornfontein between January and June 1984. COMRO (Now CSIR Miningtek) Internal report.

Vermeer, P. A., De Borst, R. (1984): Non-associated plasticity for soils, concrete and rock. Heron 29, 5–62.

Walsch, J. B., Leyde, E. E., White, A. J. A., Carragher, B. L. (1977): Stope closure studies at West Driefontein gold mine. Int. J. Rock Mech. Min. Sci. Geomech. Abstr. 14, 277–281.

Wiggill, R. B. (1965): The effects of different support methods on strata behaviour around stoping excavations. Symposium on Rock Mechanics and Strata Control in Mines. J. S. Afr. Inst. Min. Metall. 1–35.

Yang, L., Zhang, K., Wang, Y. (1996): Back analysis of initial rock stresses and time-dependent parameters. Int. J. Rock Mech. Min. Sci. Geomech. Abstr. 33, 641–645.

Author's address: Dr. D. F. Malan, CSIR Mining Technology, P. O. Box 91230, Auckland Park, 2006 South Africa.